Retrieving Optical Pulse Profiles Using a Nonlinear Optical Loop Mirror

O. Pottiez, E. A. Kuzin, and B. Ibarra-Escamilla

***Abstract*—A novel technique is proposed to characterize the power profile of short optical pulses using the transmission characteristic of a nonlinear optical loop mirror (NOLM). Under some assumptions, the power profile can be retrieved from pulse energy measurements at the NOLM output using a slow detection setup. As a fiber-based technique based on the Kerr effect, it does not require phase matching or tedious mechanical adjustments. The technique is able to characterize simultaneously pulse features from the picosecond to the nanosecond scale.**

***Index Terms*—Nonlinear optics, optical fiber devices, optical pulse measurements.**

FOR MOST applications making use of short light pulses, knowing the pulse profile is essential. Convenient measurement of pulse features whose duration is below the response time of the fastest optoelectronic devices remains, however, challenging. Several techniques use an ultrafast nonlinear optical process to achieve this task [1]–[3]. The widespread optical autocorrelation (AC) technique [1] allows us to infer pulse duration if a particular pulse profile is assumed. This technique is very useful for measuring fs pulses, and can be readily extended to allow complete pulse profile retrieval (amplitude and phase) [2], [3]. However, the free-space interferometric structure and the phase-matching requirement (if second-harmonic generation is used) impose careful beam alignment and crystal orientation and enhance sensitivity to perturbations. Moreover, mechanical scanning limits the flexibility of the measurement span. Linear techniques were also developed for complete pulse characterization, being usually simpler in processing, and requiring much less intensities than nonlinear techniques [4]–[6]. Drawbacks, however, include the need for complex electronics [4] or high-speed detection [5], [6]. Alternatives can be figured out if the shape of somewhat longer pulses is to be determined. On the other hand, although >20-ps pulses can be readily measured using 50-GHz photodetector and sampling scope, high-speed detection is expensive, and slow detection setup is preferable.

The fiber nonlinear optical loop mirror (NOLM) [7] is a versatile device that has been used for ultrafast switching, signal processing, or optical data monitoring [8]. In this letter, we propose an NOLM-based technique to retrieve the profile of short optical pulses. The Kerr effect in silica fiber is used, which requires no phase matching. All-fiber implementation avoids alignment issues, and offers high robustness and reduced cost [6]. Finally, the Sagnac architecture (in which both beams travel along the same path) improves stability.

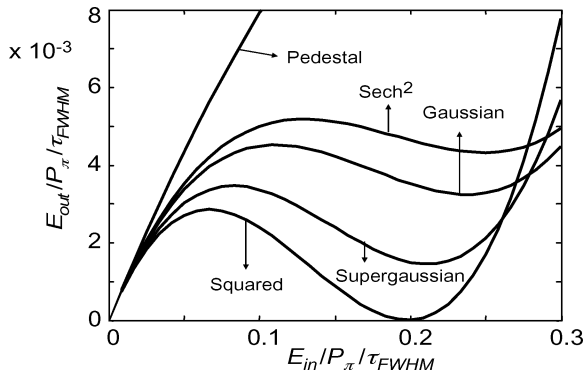

Fig. 1. Output pulse energy versus input pulse energy, for several profiles defined as curve labels (some shown in Fig. 3). Sech^2 = squared hyperbolic secant; Supergaussian = squared Gaussian. We used $\Delta\phi = \pi/5$ in (1).

The power transfer characteristic of an NOLM $T = P_{\rm out}/P_{\rm in}$ (where $P_{\rm in}$ and $P_{\rm out}$ are input and output powers, respectively) is a sinusoidal function of $P_{\rm in}$ [7]. Assuming zero minimal transmission, T writes as

$$T = K\left[\frac{1}{2} - \frac{1}{2}\cos(\pi P_{\rm in}/P_\pi - \Delta\phi)\right] \tag{1}$$

where P_π is the critical power, K the maximum transmission, and $\Delta\phi$ the phase bias. If $\Delta\phi > 0$, $T = 0$ at power $p_z = \Delta\phi P_\pi/\pi$. If the input power profile is $p(t)$, the output profile is $P_{\rm out}[p(t)]$, where $P_{\rm out}(P_{\rm in}) = T(P_{\rm in}) \times P_{\rm in}$ is the output power characteristic of the NOLM. The output pulse energy is $E_{\rm out} = \int P_{\rm out}[p(t)]dt$.

Fig. 1 shows $E_{\rm out}$ versus input pulse energy $E_{\rm in}$ for different profiles with full-width at half-maximum (FWHM) duration $\tau_{\rm FWHM}$. It appears that each profile has a specific $E_{\rm out}$ characteristic. This can be understood by considering that each pulse profile "stays" a specific time around each value of power (between 0 and peak power). For example, the "squared" profile stays at peak power over the whole pulse duration, whereas the "pedestal" profile stays most of the time well below peak power. Hence, $E_{\rm out}$ evolves much faster (increasing, decreasing, and then increasing again) in the first case than in the second ($E_{\rm out}$ monotonously increases). Note also that $E_{\rm out} = 0$ for peak power $= p_z$ only in the "squared" case, as any other profile presents skirts below the peak, where T (and $P_{\rm out}$) > 0. The specificity of $E_{\rm out}$ for each pulse shape can be exploited to retrieve the pulse profile from pulse energy measurements.

Manuscript received April 24, 2007; revised June 6, 2007. This work was supported by CONCYTEG Grant, "Estudio y Diseño de un láser de fibra óptica para generación de pulsos ultracortos."

O. Pottiez is with the Centro de Investigaciones en Óptica, León 37150, Mexico (e-mail: pottiez@cio.mx).

E. A. Kuzin and B. Ibarra-Escamilla are with the Instituto Nacional de Astrofísica, Óptica y Electrónica, Puebla 72000, Mexico.

Digital Object Identifier 10.1109/LPT.2007.902919

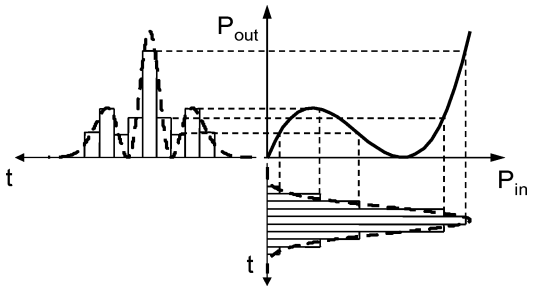

Fig. 2. Principle of vertical slicing.

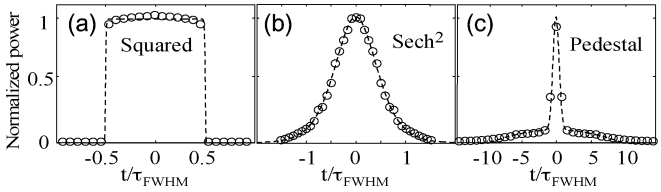

Fig. 3. Numerical results for several pulse profiles. Dashed = target, Circles = retrieved.

To introduce the principle of the technique, we first consider squared pulses. The problem then simply consists in determining the pulse duration Δt and peak power p. Pulse energy only gives the product $p\Delta t$. We consider that pulse power can be adjusted by a known coefficient a. Input pulses $ap(t)$ are then sent into an NOLM, whose T (or $P_{\rm out}$) curve is known. Pulse energy at the NOLM output is then given by $E_{\rm out}(a) = P_{\rm out}(ap)\Delta t$. If $E_{\rm out}$ is measured for two values of a, say a_1 and a_2, then $P_{\rm out}(a_1 p)/P_{\rm out}(a_2 p) = E_{\rm out}(a_1)/E_{\rm out}(a_2)$. This nonlinear equation in p allows us to determine p, if $P_{\rm out}(p)$ is not a power of p (otherwise, p cancels out from the equation). In case of multiple solutions, indetermination can be raised by measuring $E_{\rm out}$ for other two values of a. Once p is known, Δt is readily obtained through $\Delta t = E_{\rm out}(a)/P_{\rm out}(ap)$.

We now consider the general case of an unknown pulse profile. The principle described above can be generalized if we decompose the profile into N adjacent rectangular slices of duration δt (much smaller than the pulsewidth) and power p_j ($j = 1, \ldots, N$) equal to the pulse power at the center of the corresponding interval (Fig. 2). Output pulse energy is then identified to the energy of all the slices through the NOLM

$$\sum_{j=1}^{N} P_o(a_i p_j)\delta t = E_o(a_i), \qquad i = 1, \ldots, M. \tag{2}$$

Equation (2) is a system of M nonlinear algebraic equations, whose unknown quantities are the p_j ($j = 1, \ldots, N$) and δt. A necessary condition for this system to be determined is that $M \geq N + 1$. Hence, estimation of the pulse profile at N points requires at least $N+1$ measurements of $E_{\rm out}$ (for $N+1$ values of a_i). $M > N + 1$ can be used to avoid multiple solutions. Equation (2) must be solved numerically for the p_j and δt. Alternatively, $\delta t = E_{\rm out}(a_M)/\sum P_{\rm out}(a_M p_j)$ can be substituted into the first $M - 1$ equations, which are solved for the p_j only. This removes the need for an initial guess of the pulse duration, which can be calculated directly once the p_j are known.

Even if there is only one set of values p_j yielding a particular $E_{\rm out}$ characteristic, the order of succession of slices across the profile cannot be determined because the measured pulse energy contains no information about their relative timing. To raise the indetermination, we assume that the profile decreases monotonically from its peak (thus discarding possible troughs in the pulse shape), either on one side (single-sided profile), or symmetrically on both sides (symmetric profile).

The method was tested numerically for different symmetric pulse profiles (some shown in Fig. 3). T was given by (1) with $\Delta\phi = \pi/5$, yielding a zero at a moderate power $p_z = 0.2P_\pi$. The $E_{\rm out}$ curve was simulated for each profile through numerical integration of $P_{\rm out}[a_i p(t)]$. Peak powers ranged from $a_i = 0$ to $\sim 0.3P_\pi$, thus using T far below critical power. In each case, we solved (2) numerically using the least squares method (δt was substituted as described above, leaving only the p_j to determine). A symmetric profile was assumed. A Gaussian profile was chosen for the initial estimations of p_j (this choice was not critical). We used $N \approx 20$ points across the half profile, and $M - N \approx 1 - 5$. Proper convergence and profile recovery was observed for initial peak power guess in a range of $\sim$10 dB about its actual value. Although the choice of $\Delta\phi$ is not critical, it should be $\neq 0$, as otherwise $P_{\rm out}(p) \propto p^3$ for $p \ll P_\pi$, and indetermination arises, as previously mentioned (convergence is not observed in this case). For $\Delta\phi < 0$, profile is recovered but the $E_{\rm out}$ curves are more closely packed than in Fig. 1 (over the same power range). This is due to the smaller dynamic range of T at moderate power, which no longer decays to zero, but slowly grows with $P_{\rm in}$. This will reduce the robustness of profile discrimination, so that $\Delta\phi > 0$ is preferable.

It has to be stressed that the precision of the results relies on the precise knowledge of T. Numerical analysis showed that inaccuracy of parameters P_π, K, or $\Delta\phi$ affects retrieved pulse peak power, duration, or shape. As to amplitude noise, it will modify the $E_{\rm out}$ characteristic if energy is measured after averaging over many pulses in a train. Simulations show, however, that the profiles are not severely distorted for relative (Gaussian) noise magnitude up to $\sim$20% if $\Delta\phi > 0$ ($\sim$5% if $\Delta\phi < 0$). The effect of noise can be avoided by performing single-shot energy measurements (detecting simultaneously one input pulse and the corresponding output pulse).

We tested the technique experimentally. The experimental setup is analogous to the one shown in [9, Fig. 1]. We used an NOLM operating through nonlinear polarization rotation (NPR) [10], including a $\sim$50/50 coupler, 500 m of highly twisted (7 turns/m) standard SMF-28 fiber, and a quarter-wave (QW) retarder at one end of the loop. Fiber twist prevents NPR from averaging out due to residual birefringence [11] and makes the device environmentally stable, avoiding drifts of the transmission, a key condition for proper profile retrieval. The input signal to the NOLM was circularly polarized. Selecting the orthogonal circular component at the NOLM output yields the T characteristic given by (1), with $P_\pi \approx 30$ W, $K = 1/2$, and $\Delta\phi$ adjusted by the QW angle α [12]. Input and output pulses were detected with two InGaAs 1-GHz photodetectors.

We adjusted α to have minimum T at small $P_{\rm in}$. We measured T using nanosecond (ns) optical pulses from a distributed-feedback laser diode emitting at 1549 nm, biased below threshold and directly modulated by ns squared current pulses at 100 Hz. The optical pulses were amplified by an erbium-doped fiber amplifier and launched into the NOLM.

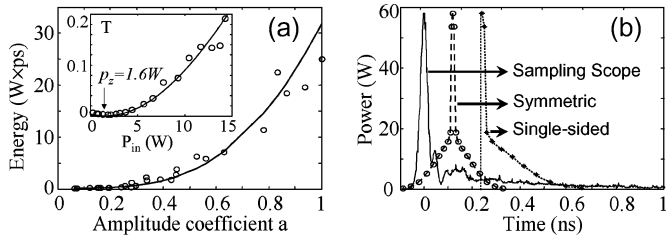

Fig. 4. (a) $E_{\rm out}$ characteristic and NOLM transmission (inset): dots = experiment, lines = fit (inset) and $E_{\rm out}$ recalculated from retrieved profile; (b) pulse profiles (shifted for better readability).

Input and output pulses were monitored on a two-channel 500-MHz oscilloscope (in average mode), allowing us to resolve pulse profiles. We measured T between 0 and $\sim$15 W by adjusting the current pulses (Fig. 4(a), inset). Insertion loss of the output polarizer is included in T. Fitting experimental data led to $\Delta\phi = 0.054\pi$. Minimal $T > 0$, which does not hinder from proper profile retrieval.

We applied the technique to characterize pulses from a figure-eight fiber laser (F8L). Fig. 4(b) (solid) shows the pulse measured with a fast photodetector (10-GHz specified bandwidth) and a 20-GHz sampling scope in averaged mode. The curve shows a $\sim$30-ps pulse followed by a $\sim$1-ns tail. This measurement determines the tail extension, but not the pulse duration, due to the bandwidth limitation of this setup. Pulse duration was measured through second-harmonic AC, which yielded $\tau_{\rm FWHM} \approx 22$ ps (assuming Gaussian pulse). The AC trace presented a substantial background, to be related with the tail of the waveform. However, its duration could not be estimated using the autocorrelator, due to its limited scanning range. A precise assessment of the waveform thus required both scope and AC measurements. These measurements also showed that the profile did not vary significantly with the mode-locked laser pump power. Pulses from the F8L were launched into the NOLM. Due to large amplitude noise affecting the pulses, input and output were monitored simultaneously, using a two-channel 500-MHz oscilloscope in single-shot mode (triggered off the input). Amplitude noise was high enough to select the input pulse power over a wide range, simply by adjusting the trigger level (in the case of stable pulses, an adjustable attenuator must be used at the NOLM input). For each value of input power, $E_{\rm out}$ was measured by integrating the impulse response of the output pulse on the scope (Fig. 4(a), circles). A Gaussian profile was used as initial waveform estimate. We used $N = 25$ and $M - N = 5$. The profiles retrieved under symmetric or single-sided assumptions are shown in Fig. 4(b), and the $E_{\rm out}$ recalculated using these values is shown in Fig. 4(a) (solid). The waveform includes a $\sim$20-ps pulse and a wide pedestal about twice shorter and higher than the tail observed on the sampling scope. This waveform is quite close to the expected profile, given the precision of measurements. However, the technique does not determine the position of the pulse in the waveform. The pulse peak power could not be estimated using the sampling scope, due to the large noise. In contrast, our technique allowed us to estimate that the highest pulses reach $\sim$60 W of peak power at the F8L output ($\sim$ 13 W into the NOLM).

For ultrashort pulses, performances will be degraded by dispersion and nonlinear effects in the NOLM. The soliton effect can be avoided if dispersion is normal, and pulses down to a few picoseconds (ps) can be characterized. As far as peak power remains moderate, stimulated Raman or Brillouin scattering can be avoided. For sub-ps pulses, higher order dispersion and nonlinear effects like self-steepening and intrapulse Raman scattering are at play, making the technique unreliable.

In conclusion, we proposed a technique to characterize the temporal power profile of short pulses, which relies on pulse energy measurements through an NOLM using moderate input peak powers. Adjustment of the transmission is not very critical for proper operation, although this characteristic must be known with precision. The technique is applicable to a wide range of pulse durations, from a few ps to a few ns, without any modification in the setup. Only low-frequency detection is needed, making the technique affordable. The profile of monotonous and symmetric pulses can be retrieved without ambiguity. Although the temporal sequence of features in complex waveforms cannot be restored, valuable information is retrieved, like duration, peak power, and the temporal distribution of instantaneous power across the pulse. This technique could complement conventional techniques for characterizing short and ultrashort pulses.

REFERENCES

[1] J.-C. Diels and W. Rudolph, *Ultrashort Laser Pulse Phenomena. Fundamentals, Techniques, and Applications on a Femtosecond Time Scale*. San Diego, CA: Academic, 1996, ch. 8.

[2] D. J. Kane and R. Trebino, "Characterization of arbitrary femtosecond pulses using frequency-resolved optical gating," *IEEE J. Quantum Electron.*, vol. 29, no. 2, pp. 571–579, Feb. 1993.

[3] J. W. Nicholson, J. Jasapara, W. Rudolph, F. G. Omenetto, and A. J. Taylor, "Full-field characterization of femtosecond pulses by spectrum and cross-correlation measurements," *Opt. Lett.*, vol. 24, pp. 1774–1776, 1999.

[4] I. Kang, C. Dorrer, and F. Quochi, "Implementation of electro-optic spectral shearing interferometry for ultrashort pulse characterization," *Opt. Lett.*, vol. 28, pp. 2264–2266, 2003.

[5] N. K. Berger, B. Levit, V. Smulakovsky, and B. Fisher, "Complete characterization of optical pulses by real-time spectral interferometry," *Appl. Opt.*, vol. 44, pp. 7862–7866, 2005.

[6] P. Kockaert, J. Azaña, L. R. Chen, and S. LaRochelle, "Full characterization of uniform ultrahigh-speed trains of optical pulses using fiber Bragg gratings and linear detectors," *IEEE Photon. Technol. Lett.*, vol. 16, no. 6, pp. 1540–1542, Jun. 2004.

[7] N. J. Doran and D. Wood, "Nonlinear optical loop mirror," *Opt. Lett.*, vol. 13, pp. 56–58, 1988.

[8] R. Adams, M. Rochette, T. T. Ng, and B. J. Eggleton, "All-optical in-band OSNR monitoring at 40 Gb/s using a nonlinear optical loop mirror," *IEEE Photon. Technol. Lett.*, vol. 18, no. 3, pp. 469–471, Feb. 1, 2006.

[9] B. Ibarra-Escamilla *et al.*, "Experimental investigation of the nonlinear optical loop mirror with twisted fiber and birefringence bias," *Opt. Express*, vol. 13, pp. 10760–10767, 2005.

[10] E. A. Kuzin, N. Korneev, J. W. Haus, and B. Ibarra-Escamilla, "Theory of nonlinear loop mirrors with twisted low-birefringence fiber," *J. Opt. Soc. Amer. B*, vol. 18, pp. 919–925, 2001.

[11] T. Tanemura and K. Kikuchi, "Circular-birefringence fiber for nonlinear optical signal processing," *J. Lightw. Technol.*, vol. 24, no. 11, pp. 4108–4119, Nov. 2006.

[12] O. Pottiez, E. A. Kuzin, B. Ibarra-Escamilla, and F. Méndez Martínez, "Easily tuneable nonlinear optical loop mirror including low-birefringence, highly twisted fibre with invariant output polarisation," *Opt. Commun.*, vol. 229, pp. 147–159, 2004.